ELSEVIER

Electrochemistry Communications 3 (2001) 274–280

electrochemistry communications

www.elsevier.nl/locate/elecom

Ion and water transports in Prussian blue films investigated with electrochemical quartz crystal microbalance

Ilwhan Oh, Hochun Lee, Haesik Yang, Juhyoun Kwak *

Department of Chemistry, Korea Advanced Institute of Science and Technology (KAIST), 373-1 Kusong-dong, Yusong-gu, Taejon 305-701, South Korea

Received 12 February 2001; received in revised form 23 February 2001; accepted 23 February 2001

Abstract

Water and ion transport in electrochemically prepared Prussian blue (PB, Iron(III) hexacyanoferrate(II)) films has been investigated with the electrochemical quartz crystal microbalance (EQCM) and the electrochemical/electrogravimetric impedance techniques. It is shown that the freshly prepared PB film is highly hydrated and that it undergoes an irreversible mass change during the first cathodic scan. The latter result supports the previously proposed structural reorganization scheme of the PB film from the insoluble form $Fe_4[Fe(CN)_6]_3 \cdot 6H_2O$ to the soluble form $MFeFe(CN)_6$ (M is a monovalent cation). It is also shown that, during the first cathodic scan, a substantial amount of water is excluded from the PB film. After the structural reorganization, ion transport during the redox reaction of the PB film is cation-dominant with a small fraction of accompanying water transport.

Keywords: Electrochemical quartz crystal microbalance; Impedance spectroscopy; Mass transport; Prussian blue

1. Introduction

Among various kinds of metal hexacyanometallate films, the Prussian blue (PB, ferric ferrocyanide) film [1–5] has been investigated most extensively, because it is easily prepared on the electrode and it can be applied to electrochromic device [6–8], battery [9–11], ion selective sensors [12,13], and electrocatalysis [14–16]. Many electrochemical studies of the PB film have been directed to the verification of the stoichiometry and the understanding of the mass transport behavior during the redox reaction of the PB film. Two stoichiometries have been reported for the chemically prepared PB film, namely the insoluble form $Fe_4[Fe(CN)_6]_3 \cdot 6H_2O$ and the soluble form $KFeFe(CN)_6$. The redox reaction of the soluble form [2] is

$$KFe^{III}[Fe^{II}(CN)_6] + e^- + K^+ \rightarrow K_2Fe^{II}[Fe^{II}(CN)_6] \quad (1)$$

and that of the insoluble form [5] is

$$Fe_4^{III}[Fe^{II}(CN)_6]_3 + 4e^- + 4K^+ \rightarrow K_4Fe_4^{II}[Fe^{II}(CN)_6]_3 \quad (2)$$

Based on the observation of the absorption spectral change of the PB film, Rosseinsky et al. [17,18] proposed that the electrochemically prepared PB film changes irreversibly from the insoluble form to the soluble form by the electrochemical reduction. On the other hand, it is known that the PB film has zeolitic structure and contains ions or water molecules at the interstitial sites. The PB film is highly hydrated in an aqueous solution and the degree of hydration affects electric conductivity [19].

In order to study the ion and solvent transport behavior during the redox reaction of a film, the electrochemical quartz crystal microbalance (EQCM) has been widely used [20,21]. The comparison between mass change (ΔM) and current (I) gives important information on the identity of charge compensating species. Moreover, when isotopically labeled solvent is used, the contributions of ion and solvent to the total mass transport can be separated [22].

Along with the EQCM technique, the electrochemical and electrogravimetric impedance techniques have been also utilized. While the electrochemical impedance

* Corresponding author. Tel.: +82-42-869-2833; fax: +82-42-869-2810.

E-mail address: jhkwak@cais.kaist.ac.kr (J. Kwak).

1388-2481/01/$ - see front matter
PII: S1388-2481(01)00144-8

technique [23–25] measures the current response to the small potential perturbation, the electrogravimetric impedance technique [26,27] measures the mass change response. The comparison between the electrochemical and electrogravimetric impedance responses gives more useful information on ion and solvent transport [28–30].

In this work, water and ion transport in the PB film was investigated with the cyclic EQCM technique and electrochemical/electrogravimetric impedance techniques. The mass transport behavior during the electrodeposition and the structural reorganization of the PB film was studied in H_2O and D_2O solutions in order to determine the degree of hydration of the PB film and to verify the irreversible structural reorganization of the PB film from the insoluble form to the soluble form. During the redox cycle, the mass transport behavior in solutions containing different cations was also investigated in order to determine the species involved in the mass transport of the PB film. Though PB is oxidized to Prussian white (PW), we focused on the reaction between PB and Everitt's salt (ES) due to the stability and reversibility of PB and ES.

2. Experimental

$FeCl_3$ (anhydrous) and $K_3Fe(CN)_6$ (99.7%) were purchased from Sigma; KNO_3 (99%), $RbNO_3$ (99.7%), $CsNO_3$ (99.99%), and $NaNO_3$ (99%) from Aldrich; HNO_3 and NH_4Cl (98%) from Junsei. All reagents were used as received without further purification. Solutions were prepared with doubly distilled water.

The details of the experimental setup for the EQCM technique, the electrochemical impedance technique, and the electrogravimetric impedance technique were same as that previously reported [28]. A single-compartment three-electrode cell was used with a Ag/AgCl/3 M NaCl reference electrode and a platinum counter electrode. The working electrode was a 6 MHz AT-cut quartz crystal coated with a thin gold film (Inficon, NY). The area of solution contact was approximately 0.32 cm^2. In our previous report [30], using the electromechanical impedance technique, it was shown that the morphology change of PB films is so insignificant that mass change can be obtained from the resonance frequency without considering the morphology change of PB film in organic solvents. The measured sensitivity of our quartz crystal is 4.42 ng/Hz [28]. The electrode potentials are reported with respect to Ag/AgCl/3 M NaCl. All experiments were conducted at room temperature.

The PB film was grown on the gold substrate by applying a constant potential of 0.6 V in the solution of 20 mM $FeCl_3$, 20 mM $K_3Fe(CN)_6$, 0.5 M KNO_3, and 0.01 M HNO_3. Two separately prepared solutions of ferric ion and ferricyanide were mixed just before deposition to minimize the spontaneous formation of precipitate. The mixed solution exhibited the reddish-brown color due to the formation of the ferriferricyanide complex [31]. The deposited amount was controlled by the consumed charge (usually $Q_{dep} = 10$ mC/cm^2). Then all electrodes were washed with distilled water, followed by rinse with the electrolyte solution to be used in the next experiments. After immersion in the electrolyte solution, a constant potential (usually 0.6 V) was applied to the electrode for about 2 min to reach the equilibrium states.

3. Results and discussion

3.1. Electrodeposition of the PB film

The PB film is electrodeposited onto the gold electrode at constant potential of 0.60 V. Fig. 1 shows the relation between the charge change (ΔQ) and the mass change (ΔM) during the electrodeposition of the PB film. A good linearity between ΔQ and ΔM is observed except at the initial stage of the electrodeposition, which indicates that the composition of the deposit is quite uniform throughout the electrodeposition process. From the slope of the $\Delta Q - \Delta M$ plot, the average molar mass is defined as the mass change per 1 mol of electrons

$$W'_{dep} = F\frac{\Delta M}{\Delta Q}, \tag{3}$$

where F is Faraday constant. W'_{dep} can be obtained by least-square fitting of ΔM and ΔQ over the linear range

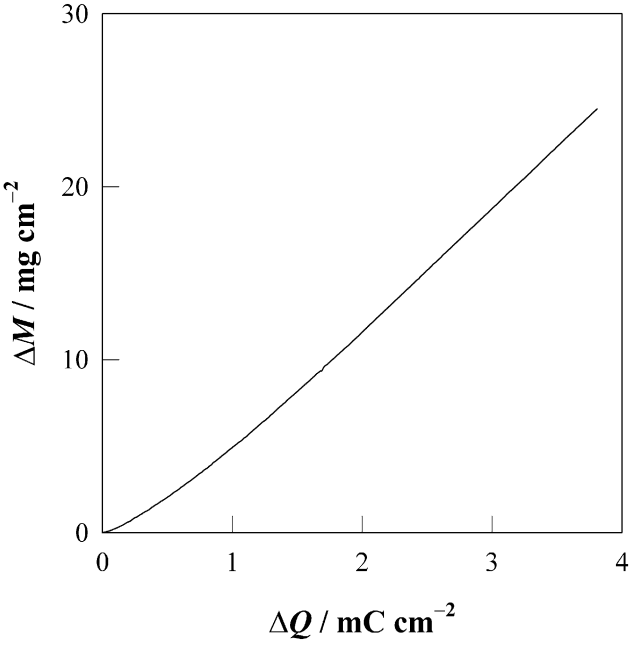

Fig. 1. Mass change (ΔM) vs charge change (ΔQ) diagram during the potentiostatic electrocrystallization of PB at $E = 0.6$ V on gold electrode in the acidic solution containing $Fe^{3+} + Fe(CN)_6^{3-}$.

(1–4 mC/cm^2 region). The value of W'_{dep} for the PB electrodeposition is determined to be 650 ± 27 g/mol, which is close to the previously reported ones of 643.5 g/mol [32] and 573 g/mol [33]. The composition of the initially deposited film is that of the insoluble-form PB, as Lundgren and Murray [34] showed by the energy dispersive spectroscopy (EDS) elemental analysis. Moreover, powder neutron diffraction study of the chemically prepared PB film [35] revealed that the PB film contains a number of water molecules. Assuming that the cathodic current is consumed entirely for the electrodeposition of the insoluble-form PB, $Fe_4[Fe(CN)_6]_3$, the degree of hydration can be determined from the difference between the W'_{dep} value and the molar mass of $Fe_4[Fe(CN)_6]_3$ (which is 288 g/mol because deposition of $Fe_4[Fe(CN)_6]_3$ involves reduction of three ferricyanide Fe(III) atoms). It is determined that 56% (w/w) of the fresh PB film is water, which shows that the electrodeposited PB film absorbs substantial amount of water. Though the degree of hydration seems quite large, we note that the crystallographic unit cell of insoluble PB is hollow and quite large (10.2 Å). Additionally, it is known that the electrodeposited PB forms a complex three-dimensional network [7], which might contain co-precipitated or occluded ions, water, and hydrolyzed ferrocyanide.

In order to confirm the water content, the PB film is deposited in D_2O solution (H/D ratio less than 1%). Then W'_{dep} value is increased to 700 ± 21 g/mol. Assuming that initially deposited film is composed of only the insoluble form, the solvent contributions to W'_{dep} values in H_2O and D_2O were 360 and 410 g/mol, respectively. The ratio 360/410 is very close to $W_{H_2O}(=18)/W_{D_2O}(=20)$, which evidently shows that the degree of hydration of the fresh PB film has been determined correctly.

3.2. Structural reorganization of the fresh PB film

Though the PB film has been studied extensively, even the stoichiometry of the PB film has been the subject of controversy [2,5]. Rosseinsky et al. [17] suggested that the insoluble-form PB film transforms into the soluble form by the first cathodic scan after deposition. Lundgren and Murray [34] proved that the transformation actually occurs by measuring potassium content in the PB film before and after the first cathodic scan. During the structural reorganization, ferric ions exit and potassium ions enter the PB film. The structural reorganization is not quantitative and both insoluble and soluble forms of PB are expected to exist together in the cyclically reduced film.

Fig. 2 shows the cyclic voltammogram and the EQCM response of the PB film ($Q_{dep} = 10$ mC/cm^2) in 0.5 M KNO_3. There is a significant difference between the first and the second scan. After the second scan, virtually identical current and mass responses are observed. As shown in Fig. 2(b), a substantial mass loss is observed after the first cathodic scan, which implies that an irreversible process occurs during the first cathodic scan. The mass change for the subsequent scans is almost reversible. Feldman and Melroy [32] assumed the following structural reorganization scheme:

$$Fe_4[Fe(CN)_6]_3 \cdot 6H_2O + 3M^+ \rightarrow 3MFeFe(CN)_6 + Fe^{3+} + 6H_2O \quad (4)$$

where M is the monovalent electrolyte cation. In Fig. 2(b), an abrupt decrease of the mass of the film was observed at ca. 0.2 V during the first cathodic scan. This decrease in mass can be attributed to the exit of the water molecules and the ferric ions in the PB film.

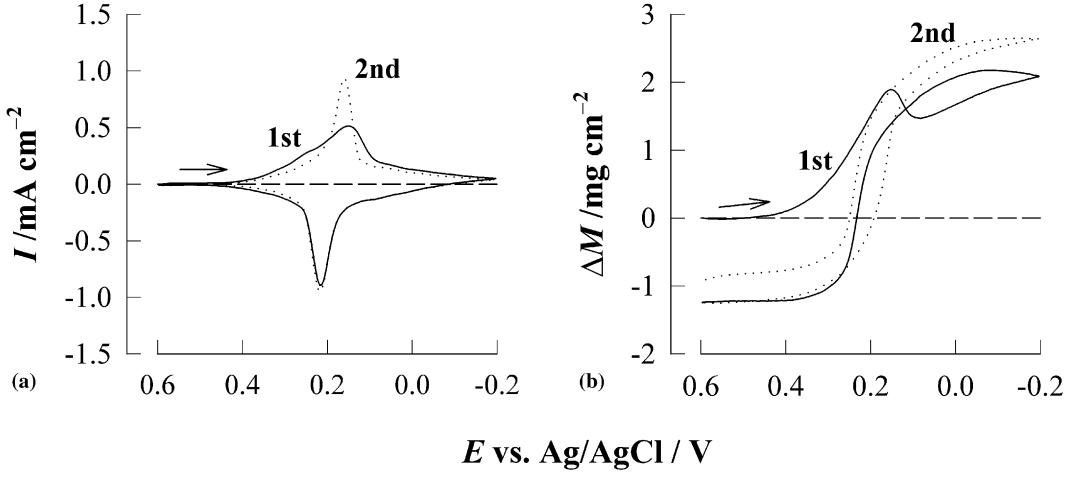

Fig. 2. (a) Cyclic voltammogram and (b) mass change diagram during the first two cyclic scans of PB in 0.5 M KNO_3 ($Q_{dep} = 10$ mC/cm^2, scan rate = 10 mV/s).

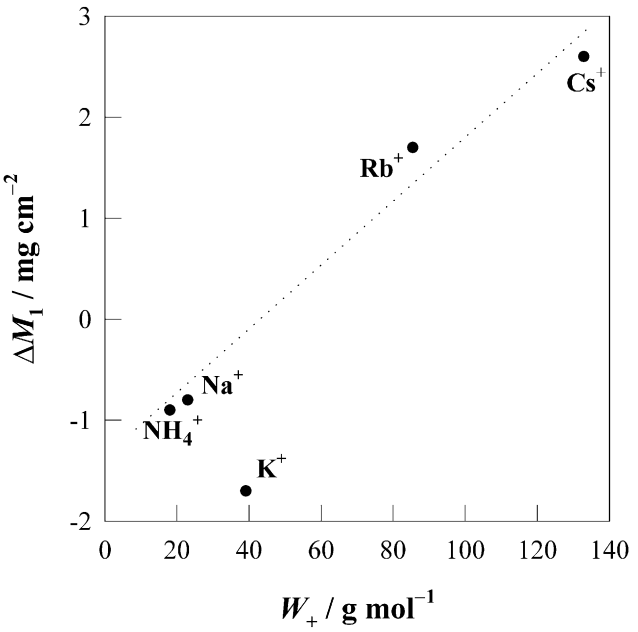

Fig. 3. Irreversible mass change (M_1) vs molar mass of cation (W_+) diagram of PB after the first scan in 0.5 M solutions of NO_3^- (Cl^- for NH_4^+) and various kinds of cations (Q_{dep} = 10 mC/cm^2, scan rate = 10 mV/s).

Fig. 3 shows the trend of the irreversible mass change after the first scan in 0.5 M NH_4Cl, $NaNO_3$, KNO_3, $RbNO_3$, and $CsNO_3$. As the molar mass of cation (W_+) increases, the irreversible mass change tends to increase as well, as expected from Eq. (4). Moreover, the linear relationship in Fig. 3 indicates that the degree of structural reorganization is fairly independent of the nature of electrolyte cation. However, the mass change in a K^+-containing solution shows a negative deviation from the linear trend. That means the degree of structural reorganization is smaller in a K^+-containing solution. This result coincides with Lundgren and Murray's observation [34] that the ratio of the first and the second cathodic charges ($\Delta Q_2/\Delta Q_1$) in a K^+-containing solution differs significantly from those in other cation-containing solutions, where $\Delta Q_2/\Delta Q_1$ was interpreted as a measure of the extent of structural reorganization.

To find out the extent of the water transport during the first scan, the PB film, which is deposited in D_2O solution, is cathodically scanned in 0.5 M KNO_3/D_2O solution (Fig. 4). Although D_2O is only 11% heavier than H_2O, a dramatic change in mass response is observed in Fig. 4(b). On the other hand, the cyclic voltammograms in H_2O and D_2O solutions (Fig. 4(a)) show that the electrochemical processes in H_2O and D_2O are nearly identical, though a slight peak shift towards positive potential is observed in D_2O solution. Therefore, this substantial variation in the mass change response is not due to the difference in the nature or the extent of the irreversible structural reorganization processes in H_2O and D_2O solutions. This large variation of the mass change response in D_2O solution proves the structural reorganization of the PB film in which the direction of water transport is opposite to that of the net ion transport (K^+ and Fe^{3+}). The amount of water transport during the structural reorganization can be obtained from the mass change responses in H_2O and D_2O solutions in Fig. 5 [8]

$$\frac{\Delta M'_{H_2O}}{W_{H_2O}} = \frac{\Delta M_{D_2O} - \Delta M_{H_2O}}{W_{D_2O} - W_{H_2O}} \quad \text{or}$$
$$\Delta M'_{H_2O} = \frac{W_{H_2O}}{W_{D_2O} - W_{H_2O}} (\Delta M_{D_2O} - \Delta M_{H_2O}), \tag{5}$$

where $\Delta M'_{H_2O}$ is the water loss during the structural reorganization in H_2O solution, and ΔM_{D_2O}(= -2.7 μg/cm^2) and ΔM_{H_2O}(= -1.2 μg/cm^2) are the net mass changes in D_2O and H_2O solutions, respectively.

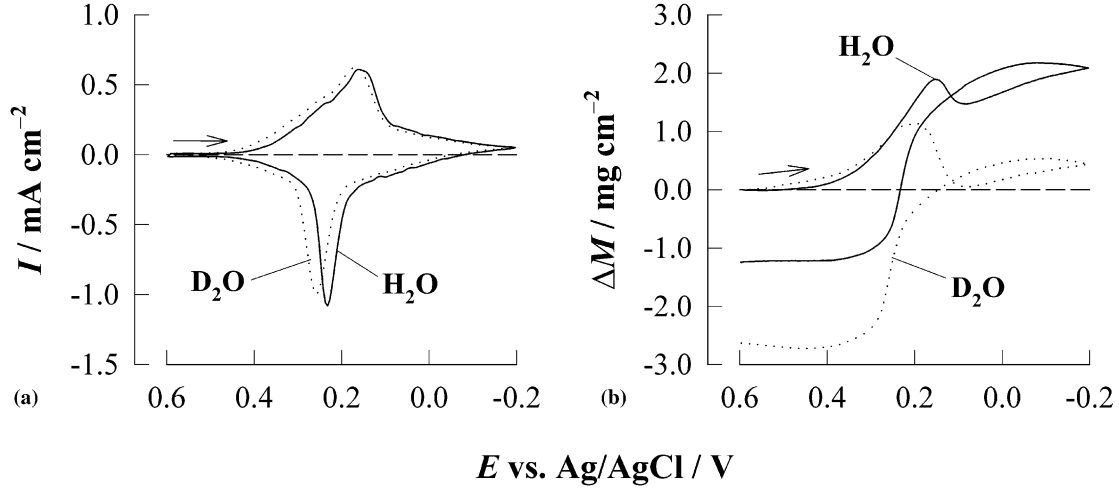

Fig. 4. (a) Cyclic voltammogram and (b) mass change diagram of PB in 0.5 M KNO_3/H_2O (solid line) and KNO_3/D_2O (dotted line) (Q_d = 10 mC/cm^2, scan rate = 10 mV/s).

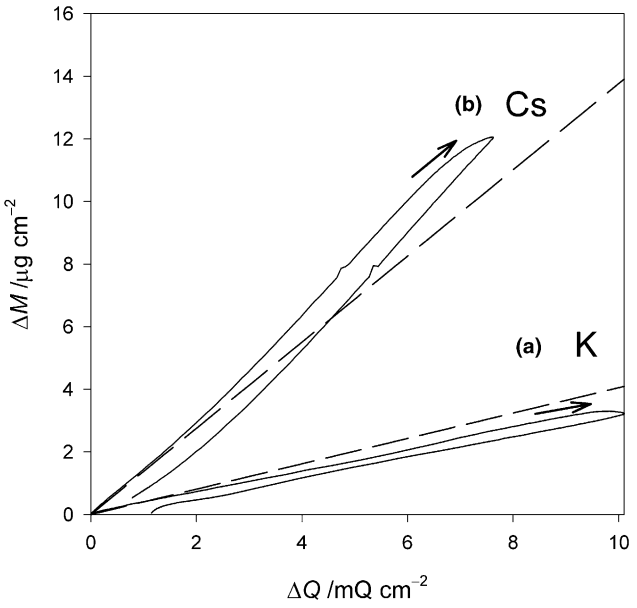

Fig. 5. Mass change (ΔM) vs charge change (ΔQ) diagrams of PB in (a) 0.5 M KNO_3 and (b) 0.5 M $CsNO_3$. The dotted lines are drawn according to $\Delta M = -(W_+/F)\Delta Q$, where W_+ is the molar mass of cation. The arrows indicate the cathodic scan. $Q_{dep} = 10$ mC/cm^{-2}, scan rate = 10 mV/s.

$\Delta M'_{H_2O}$ is about -13.5 μg/cm^2, which corresponds to about 36% of the initial water content (ca. 38 μg/cm^2) in 10 mC/cm^2 PB film. The dehydration is likely to be caused by the entrance of K^+ from the electrolyte solution into the PB cage. This result also supports the above observation that a substantial amount of water molecules are entrapped in the freshly prepared PB film.

3.3. Mass transport in the steady-state

After the structural reorganization at the first cathodic scan, the PB film showed little variation in the cyclic voltammogram and the cyclic mass change response at the subsequent scans in solutions containing NH_4Cl, $NaNO_3$, KNO_3, $RbNO_3$, and $CsNO_3$.

Fig. 5 shows the charge change (ΔQ) vs the mass change (ΔM) plots for the PB films in 0.5 M KNO_3 and in 0.5 M $CsNO_3$. Among the measurements in various monovalent cations, K^+ and Cs^+ cases are shown because they have contrary water co-transport behaviors as described below. The dotted lines are for the ideal cation perm-selective ion transports, which are drawn according to

$$\Delta M = -(W_+/F)\Delta Q, \tag{6}$$

where W_+ is the molar mass of cation. If only cation transport takes place, ΔM–ΔQ plot would match exactly with the dotted line. However, when the average molar mass of the charge compensating species is smaller than W_+, ΔM–ΔQ plot becomes smaller than the dotted line (K^+ case in Fig. 5) and vice versa (Cs^+ case in Fig. 5). The considerable mismatch of the ΔM–ΔQ plot and the dotted line in Fig. 5 indicates that cation transport in the PB film is accompanied by the transport of other chemical species. On the other hand, a fairly linear relationship between the ΔM and ΔQ plots was observed over the entire potential range in all electrolytes. This implies that the identity of the mass transport species is nearly invariant over the entire potential range. By fitting the ΔM and ΔQ plots over the potential range, the W' value in each electrolyte can be determined, as shown in Table 1. In order to determine the precision of the W' values obtained by the above procedure, measurements are conducted for the five separately prepared PB in 0.5 M KNO_3. The average values of W' during the second cathodic and anodic scans are 31 ± 1.2 (3.9%) g/mol and 33 ± 1.9 (5.8%) g/mol, respectively.

Fig. 6 shows the electrochemical capacitance ($\Delta Q/\Delta E$) and the electrogravimetric capacitance ($\Delta M/\Delta E$) plots for the PB films in 0.5 M KNO_3 and in 0.5M$CsNO_3$. The ($\Delta M/\Delta E$) plot was normalized by a factor of (F/W') for comparison, i.e., $(\Delta M/\Delta E)_n = (F/W')(\Delta M/E)$ without consideration of water transport ($W' = W_+$) to show the considerable contributions of non-cationic species to the net mass transport. If only cation transport takes place, the electrochemical semicircle ($\Delta Q/\Delta E$) would coincide exactly with the normalized electrogravimetric semicircle $(\Delta M/\Delta E)_n$. However, when the average molar mass of the transporting species is smaller than that of the cation, the $(\Delta M/\Delta E)_n$ plot becomes smaller than the ($\Delta Q/\Delta E$) plot (Fig. 6(a)) and vice versa (Fig. 6(b)). As in cyclic

Table 1
Average molar masses (W') of PB in 0.5 M NH_4Cl, $NaNO_3$, KNO_3, $RbNO_3$, and $CsNO_3$, obtained by least-square fitting of M and Q (Fig. 5) or C^M and C^Q (Fig. 6)[a]

Cation	W_+	Cyclic EQCM		Impedance W'
		Cathodic W'	Anodic W'	
NH_4^+	18	13	12	13
Na^+	23	25	23	28
K^+	39	31	33	34
Rb^+	85	84	75	72
Cs^+	133	161	167	174

[a] $Q_d = 10$ mC/cm^2, scan rate = 10 mV/s.

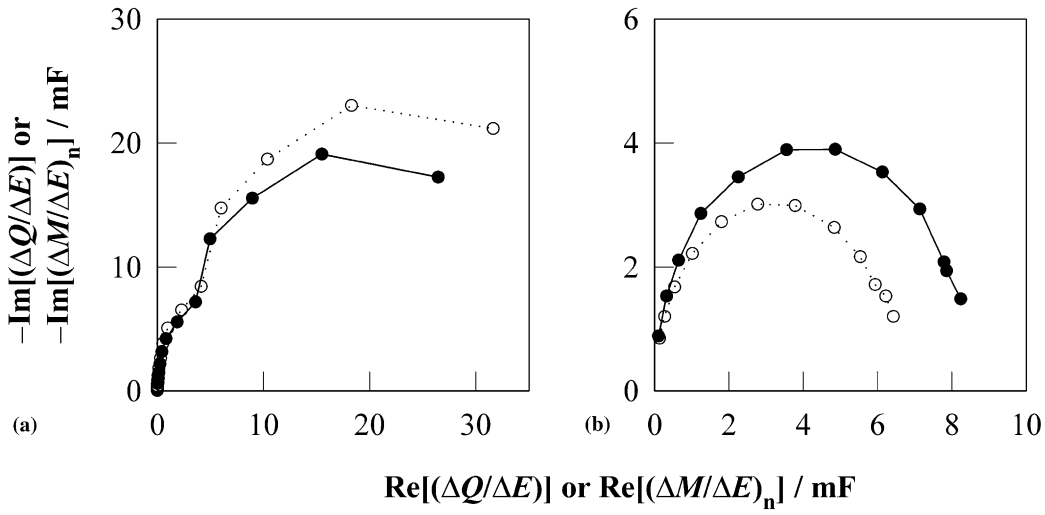

Fig. 6. Electrochemical capacitance ($\Delta Q/\Delta E$; solid line) and normalized electrogravimetric capacitance ($(\Delta M/\Delta E)_n = -(F/W_+)(\Delta M/\Delta E)$; dotted line) plots for PB (a) in 0.5 M KNO_3 at $E = 0.20$ V and (b) in 0.5 M $CsNO_3$ at $E = 0.30$ V ($Q_{dep} = 10$ mC/cm^2, scan rate = 10 mV/s).

experiments (Fig. 5), the considerable mismatch of the $(\Delta M/\Delta E)$ and $(\Delta Q/\Delta E)_n$ plots in Fig. 6 indicates that cation transport in the PB film is accompanied by the transport of other chemical species. By fitting the $(\Delta M/\Delta E)$ and $(\Delta Q/\Delta E)$ plots over the whole frequency range, W' value in each electrolyte can be determined.

Table 1 shows W' values of the PB films in 0.5 M NH_4Cl, $NaNO_3$, KNO_3, $RbNO_3$, and $CsNO_3$, which are obtained by fitting of ΔM and ΔQ for the cyclic experiments, or $(\Delta M/\Delta E)$ and $(\Delta Q/\Delta E)$ for the impedance experiments. Note that W' values from the cyclic experiments are similar to those from impedance experiments despite the fact that the two techniques are independent of each other, and impedance experiment results are obtained at a specific potential while cyclic experiment results are fitted over the entire potential range.

On the other hand, it is important to verify which chemical species contributes to the mass transport of the PB film. The order of W' values in various cations follows that of W_+ values (Table 1). Moreover, in the mass change response, ΔM increases upon reduction and decreases upon oxidation in all electrolytes (Fig. 5). These results clearly show that cations play a major role in the mass transport of the PB film. The discrepancy from the cation perm-selective ion transport mode can be understood in two ways: water molecules might accompany the cation movement. That is, the water molecules hydrated to the electrolyte cation can move together, which will increase W'. This type of water co-transport was observed in polypyrrole films [28]. Conversely, the incoming cations might push out the water molecules in the PB film, which will decrease W_{avg}. As we have shown above, in the structural reorganization of the fresh PB film, the water molecules in the PB film are lost upon entrance of cations. Secondly, anion transport could also contribute to the net mass transport. However, this is less likely because anions are too large to transport into the small PB channel size of ca. 1.6 Å [6].

4. Conclusion

From the comparison between charge change and mass change responses during the electrodeposition of the PB film, it was found quantitatively that the PB film is highly hydrated and that it undergoes an irreversible mass change during the first cathodic scan, which evidently results from the structural reorganization of the PB film from the insoluble form to the soluble form. Except in KNO_3, the extent of the structural reorganization is largely independent of the nature of the electrolyte cation. Substantial amount of water molecules escapes the PB film during the structural reorganization. In the steady-state mass transport of the PB film, the identity of the transporting species is nearly invariant over the entire potential range and the electrolyte cation plays a major role in the ion transport.

Acknowledgements

This work was supported in part by the Brain Korea 21 project in 2001 and by the Korea Science and Engineering Foundation through the MICROS center at KAIST, Korea.

References

[1] V.D. Neff, J. Electrochem. Soc. 125 (1978) 886.
[2] E.D.M. Eckhoff, V.D. Neff, J. Phys. Chem. 85 (1981) 1225.
[3] K. Itaya, H. Akahoshi, S. Toshima, J. Electrochem. Soc. 129 (1982) 1498.

[4] K. Itaya, T. Ataka, S. Toshima, T. Shinohara, J. Phys. Chem. 86 (1982) 2415.
[5] K. Itaya, T. Ataka, S. Toshima, J. Am. Chem. Soc. 104 (1982) 4767.
[6] K. Itaya, K. Shibayama, H. Akahoshi, S. Toshima, J. Appl. Phys. 53 (1982) 804.
[7] K. Itaya, I. Uchida, V.D. Neff, Acc. Chem. Res. 19 (1986) 162.
[8] N. Leventis, Y.C. Chung, Chem. Mater. 4 (1992) 1415.
[9] V.D. Neff, J. Electrochem. Soc. 132 (1985) 1382.
[10] K. Honda, H.J. Hayashi, J. Electrochem. Soc. 134 (1987) 1330.
[11] N. Imanish, T. Morikawa, J. Kondo, Y. Takeda, O. Yamamoto, N. Kinugasa, T. Yamagishi, J. Power Sources 79 (1999) 215.
[12] M. Hartmann, E.W. Grabner, P. Bergveld, Sensor Actuators B 4 (1991) 333.
[13] M.R. Deakin, H. Byrd, Anal. Chem. 61 (1989) 290.
[14] K. Itaya, N. Shoji, I. Uchida, J. Am. Chem. Soc. 106 (1984) 3423.
[15] K. Ogura, I. Yoshida, Electrochim. Acta 32 (1987) 1191.
[16] A.A. Karyakin, O.V. Gitelmacher, E.E. Karyakin, Anal. Chem. 67 (1995) 2419.
[17] R.J. Mortimer, D.R. Rosseinsky, J. Chem. Soc. Dalton Trans. (1984) 2059.
[18] A. Hamnett, S. Higgins, R.S. Mortimer, D.R. Rosseinsky, J. Electroanal. Chem. 255 (1988) 315.
[19] P. Piela, P.K. Wrona, Z. Galus, J. Electroanal. Chem. 378 (1994) 159.
[20] H.J. Buser, D. Schwarzenbach, W. Petter, A. Ludi, Inorg. Chem. 16 (1977) 2704.
[21] D.A. Buttry, M.D. Ward, Chem. Rev. 92 (1992) 1355.
[22] J. Lasky, D.A. Buttry, J. Am. Chem. Soc. 110 (1988) 6258.
[23] Southampton Electrochemistry Group, Instrumental Methods in Electrochemistry, Horwood, New York, 1993 (Chapter 8).
[24] J.R. Macdonald, Impedance Spectroscopy, Wiley, New York, 1987.
[25] M.M. Musiani, Electrochim. Acta 35 (1990) 1665.
[26] D.A. Buttry, Applications of the quartz crystal microbalance to electrochemistry, in: A.J. Bard (Ed.), Electroanalytical Chemistry, vol. 17, Marcel Dekker, New York, 1991, p. 1.
[27] C. Gabrielli, B. Tribollet, J. Electroanal. Chem. 97 (1993) 4187.
[28] H. Yang, J. Kwak, J. Phys. Chem. B 101 (1997) 774.
[29] H. Yang, J. Kwak, J. Phys. Chem. B 101 (1997) 4656.
[30] H. Lee, H. Yang, Y.T. Kim, J. Kwak, J. Electrochem. Soc. 147 (2000) 3801.
[31] B.J. Feldman, O.R. Melroy, J. Electroanal. Chem. 234 (1987) 213.
[32] J.A. Ibers, N. Davidson, J. Am. Chem. Soc. 73 (1951) 476.
[33] M. Zadronecki, P.K. Wrona, Z. Galus, J. Electrochem. Soc. 146 (1999) 620.
[34] C.A. Lundgren, R.W. Murray, Inorg. Chem. 27 (1988) 933.
[35] F. Herren, P. Fischer, A. Ludi, W. Halg, Inorg. Chem. 19 (1980) 956.